Desalination and Water Treatment
www.deswater.com

17 (2010) 233–241
May

1944-3994/1944-3986
doi: 10.5004/dwt.2010.1723

Hydrogen separation membrane encapsulating Pd nanoparticles in a silica layer

Kensuke Nagata[a], Manabu Miyamoto[b], Yuichi Fujioka[a,b], Katsunori Yogo[a,b]*

[a]*Graduate School of Material Science, Nara Institute of Science and Technology, 8916-5, Takayama-Cho, Ikoma, Nara 630-0192, Japan*
[b]*Research Institute of Innovative Technology for the Earth (RITE), 9-2 Kizugawadai, Kizugawa, Kyoto 619-0292, Japan*
Tel. +81774752305; Fax +81774752318; email: yogo@rite.or.jp

Received 31 July 2009; accepted 22 November 2009

ABSTRACT

A novel composite membrane encapsulating Pd nanoparticles in a silica layer was prepared. The membrane showed H_2 selectivity in an equimolar mixture of H_2 and CO_2. The Pd nanoparticles were synthesized within a silica layer having a thickness of 1 μm. This composite structure showed good stability and could significantly reduce the amount of Pd used in the membrane.

Keywords: Hydrogen; Palladium; Mesoporous silica

1. Introduction

Palladium-based membranes for hydrogen separation have been the focus of many studies because of their potential in hydrogen purification at high temperature. Many research groups have investigated preparation of thin Pd membranes to reduce the amount of Pd required, which directly affects the membrane cost because Pd is very expensive [1,2].

To prepare a thin Pd based membrane, various preparation methods have been applied such as electroplating [3,4], electroless plating [5,6], and chemical vapor deposition [7]. Although thin Pd based membranes have shown higher permeability, thermal stress and hydrogen embrittlement significantly affect their stability.

To achieve high stability, Suda et al. reported a Pd membrane composed of a composite layer of Pd and porous substrate and with no interlayer [8]. This Pd membrane had high thermal resistance because the Pd layer did not contact the porous substrate. Tanaka et al. prepared a Pd/γ-alumina composite membrane that had no Pd outer layer [9,10]. They reported this composite membrane had good stability with hydrogen embrittlement. It is known that lattice distortion due to phase transitions is considerably suppressed when the particle size of Pd is only a few nanometers.

Therefore, the Pd nanoparticle composite membrane is a candidate for a new structural membrane with high durability and low cost. To reduce the Pd amount in the membrane and achieve high stability, the encapsulation of Pd nanoparticles in a mesoporous silica membrane was investigated in this study. Many studies have reported synthesis of metal nanoparticles and nanowires in mesoporous silica [11,12]. These metal particles have generally been synthesized in the mesoporous silica by the repeated impregnation and reduction method [13–15]. However, it is probably difficult to completely fill the mesopores by this method alone. Some researchers reported the formation of Ni nanowires in SBA-15 mesoporous channels by electroless plating [16,17]. It would be possible to fill the mesopores with metals by electroless plating.

Electroless plating of Pd was applied in this study to synthesis of a Pd encapsulated membrane. Two methods for Pd nuclei generation were studied, the amine-modification method and the counter diffusion method. Electroless plating was employed to densify the Pd nanoparticles in the mesopores and their hydrogen permeation properties were investigated.

*Corresponding author

Presented at the Fifth Conference of the Aseanian Membrane Society Aseania 2009 "Recent Progress in Membrane Science and Technology", 12–14 July 2009, Kobe, Japan.

2. Experimental

2.1. Materials

Tetraethyl orthosilicate (TEOS), colloidal silica solution 3-aminopropyltriethoxysilane (APS) and palladium acetylacetonate (Pd(acac)) were purchased from Sigma-Aldrich. Cetyltrimethylammonium bromide (CTAB), ethylenediamine-*N*,*N*,*N*′,*N*′-tetraacetic acid, disodium salt, dehydrate (EDTA) and palladium chloride ($PdCl_2$, special grade) were purchased from Wako Pure Chemical Industries Corporation. Tetraamine palladium chloride monohydrate ($Pd(NH_3)_4Cl_2{\cdot}H_2O$) was purchased from Alfa Aesar. All materials were used without further purification.

2.2. Synthesis of the mesoporous silica thin layer

The substrate used for membrane deposition was an asymmetric porous Al_2O_3 disk (ø18.5 mm, thickness 3 mm) consisting of a dense layer with an average pore diameter of 70 nm and a substrate layer with a pore diameter of 700 nm (Noritake Corporation Limited). The α-alumina substrate was first hydrophobized by a silylation agent including a bulky alkyl group, hexadecyltrichlorosilane. Hexadecyltrichlorosilane (1 mL) was mixed with 100 ml of toluene (100 mL) and the α-alumina substrate was immersed in this mixture at 323 K for more than 2 h. The α-alumina substrate was washed with toluene several times and dried at 333 K before use.

A thin mesoporous silica layer was prepared on the porous α-alumina substrate by the spin-coating method. This synthesis procedure was chosen following a previous report [18]. The synthesis solution consisted of TEOS, CTAB, ethanol and water (adjusted to pH 1.25 with hydrochloric acid) in a molar ratio of 1.0:0.1:11.8:5.0 (TEOS:CTAB:EtOH:H_2O). The silica sol was dropped onto the α-alumina substrate and the thin mesoporous silica layer was synthesized by spin coating at 4,000 rpm for 60 s. After drying at room temperature, the spin-coating process was repeated again. This coating-drying process was repeated four times. The final mesoporous silica thin membrane on the α-alumina substrate (MS/Al_2O_3) was obtained by calcination at 823 K for 6 h to remove the surfactant in the mesoporous silica layer.

2.3. Direct impregnation of Pd nuclei in the mesoporous silica membrane

Pd nuclei were directly impregnated into the mesopores using three Pd sources: 0.1 M H_2PdCl_4 aq, 0.1 M $Pd(NH_3)_4$ aq, and 0.1 M Pd(acac)/CH_3Cl. Pd/Si ratios of the Pd impregnated silica membrane were measured by X-ray photoelectron spectroscopy (XPS) and the size and dispersivity of the Pd nuclei were observed by transmission electron microscopy (TEM).

2.4. Preparation of Pd/APS/silica composite membrane

To achieve dense packing of Pd nuclei in the mesopores, amine-modification of the mesoporous silica was employed. 3-Aminopropyltriethoxysilane (APS) was chemically grafted into the mesopores of the MS/Al_2O_3. Then, Pd/APS/silica composite membranes were prepared by impregnation of Pd salt on the amine-modified mesoporous silica membrane (APS-1 and 2). The details for amine-modification were described elsewhere [18]. Then, calcination and hydrogen reduction were carried out on APS-1 at 573 K for 3 h in air and at 573 K for 3 h in a hydrogen/argon gas mixture ($H_2/Ar = 50/50$). Only hydrogen reduction was performed on APS-2.

In addition, electroless plating was carried out to densely fill the mesopores with Pd nanoparticles. The electroless plating solution consisted of palladium chloride, EDTA, aqueous ammonium solution, deionized water and hydrazine. The electroless plating solution filtered from the membrane side to the support side at room temperature for 5 h. The product was rinsed with water and dried at 343 K. The amine-functionalized mesoporous silica membrane produced after electroless plating was denoted as APS-3.

2.5. Preparation of Pd/silica composite membrane by counter diffusion methods

Pd nuclei were introduced to the mesopores using a penetrating hydrazine solution reductant from the membrane side and a H_2PdCl_4 solution Pd source from the support side. Then, electroless plating was carried out by the vacuum method. The electroless plating solution was introduced from the mesoporous silica membrane side and passed through the membrane. This membrane was denoted as CD-1.

2.6. Preparation of intermediate silica layer

A colloidal silica sol (1 wt %) was dropped onto the α-alumina substrate and an intermediate silica layer was synthesized by spin coating at 4,000 rpm for 60 s followed by calcination at 873 K for 6 h. After that, Pd impregnation, preparation of the mesoporous silica layer and electroless plating were carried out as same procedure as CD-1. This membrane was denoted as CD-2.

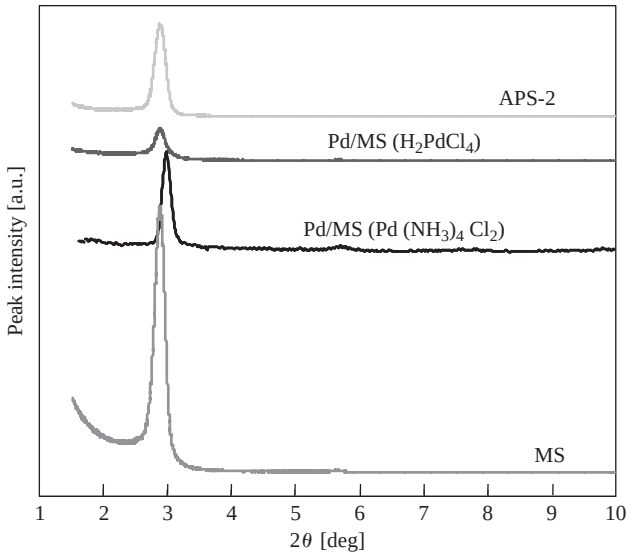

Fig. 1. XRD patterns of MS/Al_2O_3 and the Pd/MS membranes Pd$(NH_3)_4Cl_2$ and H_2PdCl_4 and APS-2.

2.7. Characterization

Structural analyses of these mesoporous silica membranes were conducted by X-ray diffraction (XRD). The Pd nanoparticle diameters of the membranes were evaluated by TEM. Surface observations and thickness measurements of the membranes were performed with scanning electron microscope energy-dispersive X-ray spectroscopy (SEM-EDX). XRD patterns were recorded from 2θ = 1.5–10° on an X-ray diffractometer (Rigaku RINT2000) using Cu Ka X-ray (40 kV and 40 mA).

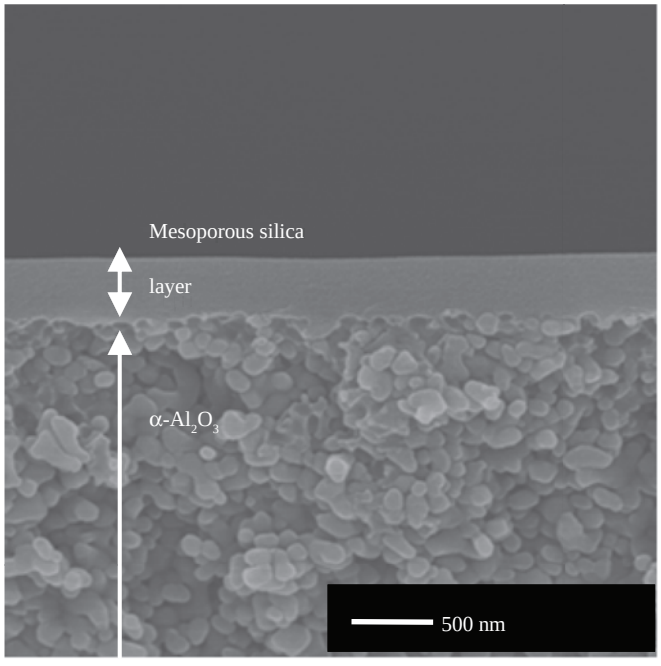

Fig. 2. SEM image of a cross sectional area of MS/Al_2O_3.

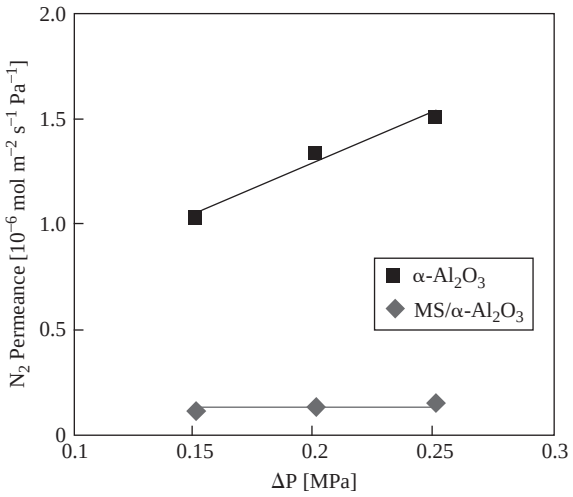

Fig. 3. The result of nitrogen single gas permeation testing with differential pressure over an α-alumina substrate and MS/Al_2O_3 at 298 K.

TEM observation was performed on a HITACHI HF-2000 electron microscope (200 kV). Membrane samples were scratched with a blade and the obtained powder was dispersed in 1 ml of ethanol. After 1 h, a few drops of suspension were deposited on a microgrid and dried in air. The microgrid was evacuated for 1 h and then observed by TEM.

SEM-EDX micrographs were obtained with a HITACHI S-5000 electron microscope (10 kV). Mesoporous silica membranes that had been broken into pieces were placed on a holder and coated with Pt-Pd by ion sputtering (HITACH E102) with a current of 15 mA at 0.05 Torr for 2 min.

XPS analyses of the membranes were carried out with an ESCA-3100 X-ray photoelectron spectrometer (Shimadzu Corporation, Japan). Analysis conditions were 8 kV and 30 mA.

Gas permeation properties were evaluated at 373 and 573 K in an equimolar feed gas of H_2 and CO_2 using a differential pressure type gas permeability device.

3. Results and discussion

3.1. Synthesis of the mesoporous silica thin layer

The MS/Al_2O_3 membrane was characterized by XRD analysis and SEM. A XRD peak at 2.88–2.90° with a d-spacing of 3.04–3.06 nm was confirmed in the XRD diffraction patterns of MS/Al_2O_3 and the Pd encapsulated membranes (Fig. 1).

This XRD peak indicates that a highly ordered mesoporous silica layer could be prepared on the

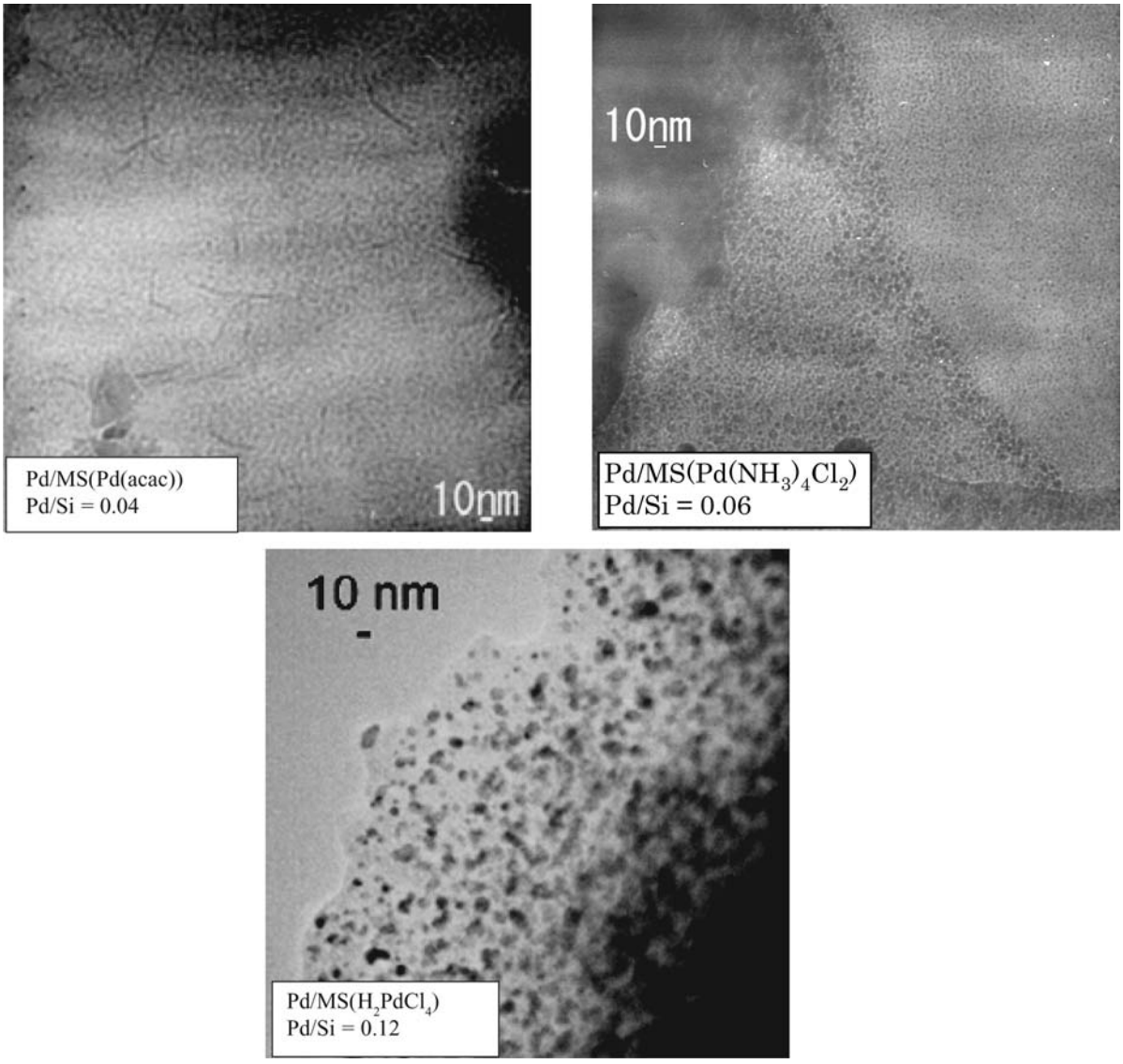

Fig. 4. TEM images of the Pd/MS membranes Pd(acac), $Pd(NH_3)_4Cl_2$ and H_2PdCl_4.

porous α-alumina substrate. The SEM image of a cross sectional area of MS/Al_2O_3 showed the mesoporous silica layer had a thickness of 0.3–0.5 μm (Fig. 2). The silylation treatment to increase hydrophobicity on the α-Al_2O_3 substrate successfully produced a thin mesoporous silica layer on the porous substrate. From gas permeation testing, the nitrogen permeance at 298 K was found to be independent of the differential pressure (Fig. 3). This result indicates that the Knudsen diffusion mechanism was dominant and MS/Al_2O_3 did not have any large cracks or pinholes.

3.2. Direct impregnation of various Pd salts into mesopores

TEM images were obtained of the Pd encapsulating membranes synthesized by direct impregnation, Pd(acac), $Pd(NH_3)_4Cl_2$ and H_2PdCl_4, and their Pd to Si ratios were measured by XPS (Fig. 4).

The silica based materials become electrically neutral at pH 2.0. The pH values for $Pd(NH_3)_4Cl_2$ aq and H_2PdCl_4 aq were 8.5 and 1.0, respectively. Therefore, $Pd(NH_3)_4^{2+}$ and $PdCl_4^{2-}$ could easily adsorb on the surface of the mesoporous silica. The Pd/Si ratio of the membrane made using H_2PdCl_4 was higher than that of the membrane by $Pd(NH_3)_4Cl_2$. The higher Pd/Si ratio might be due to the difference in solubility between $PdCl_2$ and $Pd(NH_3)_4Cl_2$. The solubility of $PdCl_2$ in water is lower than that of $Pd(NH_3)_4Cl_2$, therefore more $PdCl_2$ are likely to remain adsorbed to the silica surface after washing with water.

The size of Pd particles in the membrane made using H_2PdCl_4 was approximately 7 nm, which was larger

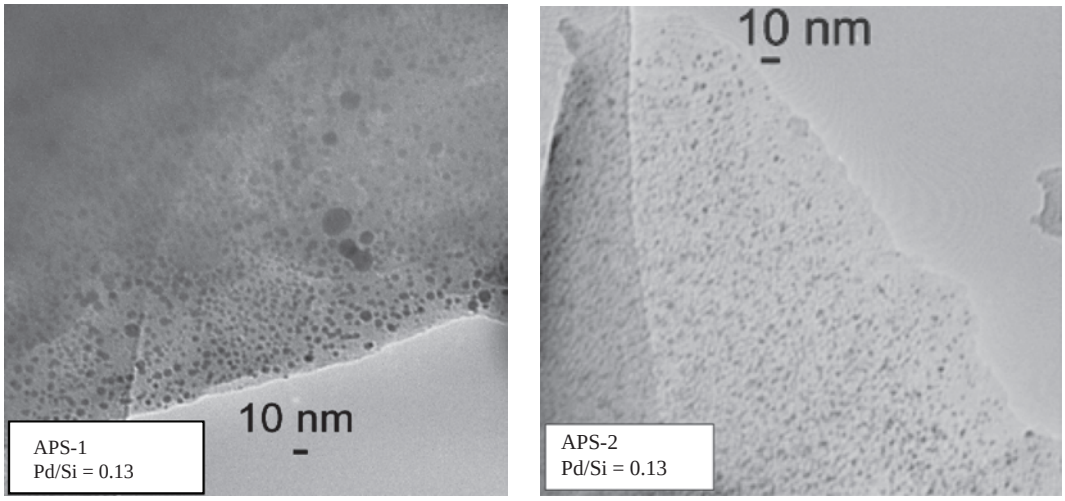

Fig. 5. TEM images of the Pd/MS membranes APS-1 and APS-2.

than with the other two Pd sources where the particle size was approximately 4 nm. Of the XRD patterns for the Pd impregnated membranes with different Pd sources, the H_2PdCl_4 membrane showed the lowest intensity peak. This indicates the strong acidity of the H_2PdCl_4 solution caused disordering of the mesostructure and the particle size became larger than the pore size. In contrast, in the case of $Pd(NH_3)_4Cl_2$, most of the Pd particles had very similar size to the pore size, suggesting Pd particles could be mainly generated within the mesopores and indeed, its XRD pattern showed high regularity of the mesoporous material.

To achieve a high density of Pd nuclei in the mesoporous silica layer, H_2PdCl_4 was used as the Pd source and amine modification of the mesoporous silica surface was employed to prevent the destruction of the ordered mesoporous structure. In addition, Pd nuclei were expected to form preferentially within the mesopores because modified amino groups can act as Pd adsorption sites.

3.3. Structure of Pd encapsulated membranes

The prepared membranes APS-1 and 2 were characterized by XRD and TEM. The main XRD peak did not shift after amine-modification and Pd impregnation (Fig. 1). This indicates the regularity of the mesoporous silica membrane was retained. Fig. 5 shows TEM images of the Pd/MS membranes APS-1 and 2. APS-1 and 2 have an average Pd particle diameter of approximately 4 nm. This particle size is smaller than that in Pd/MS and similar to the size of the mesopores,

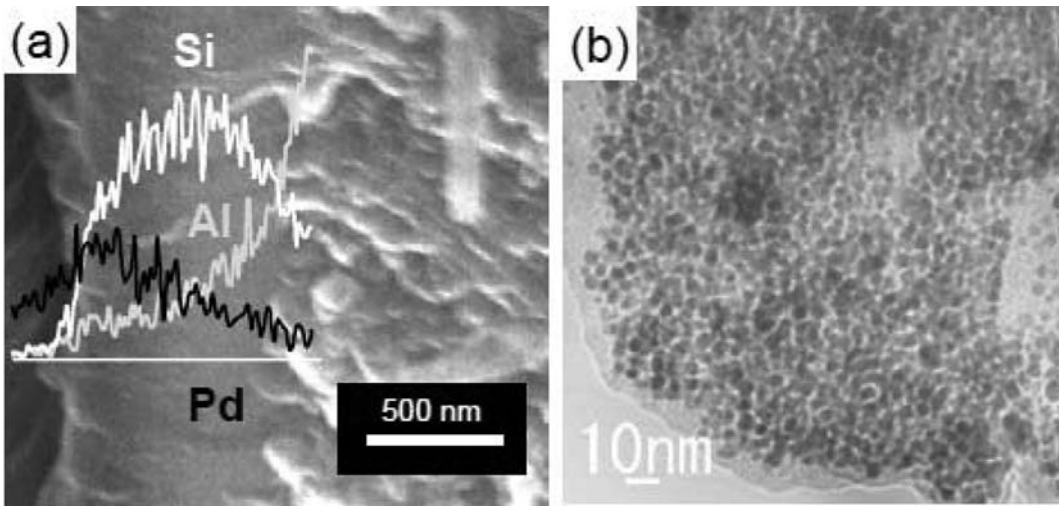

Fig. 6. SEM-EDX and TEM images of APS-3.

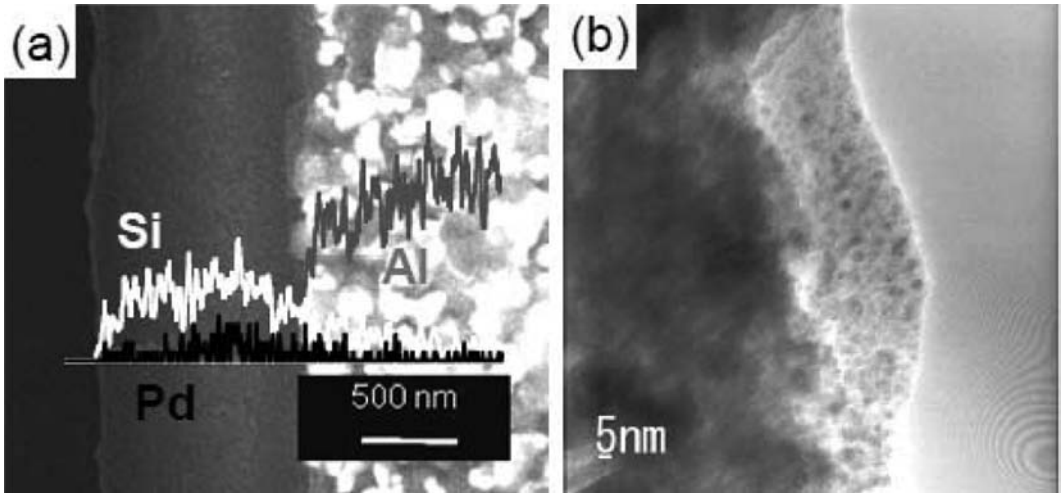

Fig. 7. SEM-EDX and TEM images of CD-1.

indicating many Pd particles were grown inside the mesopores.

In addition, the silica frame network was reinforced by APS and many periodic mesopores were present after Pd impregnation.

Thus, the amine-modification could efficiently adsorb Pd ions within the mesopores.

The structure of APS-3 was analyzed by SEM-EDX and TEM. SEM-EDX analysis of the cross sectional area showed the Pd–Si composite layer was approximately 1 μm thick (Fig. 6a) and the Pd layer was observed near the external surface of the silica layer. This indicates amine groups had reacted not only within the mesopores but also on the external surface of the silica layer, and Pd nuclei were generated around these regions. Aminosilane reagents were supplied from the membrane side and so the adsorption sites of Pd nuclei would be preferentially generated in the vicinity of the membrane surface. From the XPS depth profile analyses of APS-1, it was confirmed that Pd nuclei concentration decreased with depth. Therefore, the Pd layer was synthesized near the outer surface rather than on the internal layer.

A TEM image of the Pd/silica composite layer of APS-3 showed the Pd nanoparticles had become larger (approximately 5 nm) and more densely packed (Fig. 6b). The electroless plating could make Pd nuclei grow and Pd nanoparticles might densely pack the mesopores.

The Pd encapsulated membrane synthesized by the counter diffusion method was also characterized by SEM-EDX (Fig. 7a) and TEM (Fig. 7b). No Pd layer was observed on the outer surface of the silica layer, Pd was detected only at the region near the interface between the silica layer and porous substrate. This means Pd nuclei were preferentially synthesized near the interface because the diffusivity of substances through the porous substrate should be much larger than that through the mesopores in the silica layer. However, the size of Pd nanoparticles was the same as in the amine modification method, at approximately 5 nm. The ordered structure of the mesoporous silica layer disappeared during the Pd loading processes, including both Pd impregnation and electroless plating. This occurred because the size of the Pd nanoparticles was much larger than the pore size of the prepared mesoporous silica layer in both preparation methods. Lattice expansion due to phase transition from palladium to palladium hydride caused hydrogen embrittlement, resulting in deterioration of the membrane performance. It has been reported that smaller Pd particles of nanometer size suppress lattice expansion because hydride formation is minimal with Pd nanoparticles [19]. Therefore, this composite structure might prevent damage caused by hydrogen embrittlement. In addition, this composite structure could considerably reduce the amount of Pd metal required for the membrane.

3.4. Hydrogen permeation properties of Pd encapsulated membranes

Table 1 shows the hydrogen permeation properties of Pd encapsulated membranes. The H_2 selectivity of the mesoporous silica membrane before Pd impregnation was only 5, which shows that diffusion through the membrane was controlled by the Knudsen diffusion mechanism. This result agrees with the result of the nitrogen permeation test and the membrane had no defects larger than approximately 5 nm [20]. The Pd/MS membrane had a hydrogen selectivity of 10,

Table 1
Hydrogen permeation properties of the membranes at 573 K.

Sample name	H_2 permeance (mol m^{-2} s^{-1} Pa^{-1})	CO_2 permeance (mol m^{-2} s^{-1} Pa^{-1})	$\alpha_{H2/CO2}$
MS/Al_2O_3	2.1×10^{-6}	4.1×10^{-7}	5
Pd/MS	1.4×10^{-8}	1.2×10^{-9}	10
APS-1	1.0×10^{-7}	4.2×10^{-8}	20
APS-2	2.1×10^{-7}	4.1×10^{-9}	50
APS-3	1.9×10^{-6}	3.1×10^{-9}	610
CD-1	5.6×10^{-7}	1.9×10^{-9}	300
CD-2	1.9×10^{-7}	1.3×10^{-10}	1,500

which was double that of the Knudsen diffusion, indicating the Pd impregnation clearly enhanced the H_2 selectivity. The H_2 selectivity of APS-1 and 2 were 20 and 50, respectively, and their selectivities were much higher than that of Pd/MS. This was because the amine modification could achieve highly dispersed Pd nanoparticles in the mesopores. The lower selectivity of APS-1 compared with APS-2 would be caused by calcinations of the membrane before hydrogen reduction. These calcinations would completely decompose the modified amino groups on the wall of the mesopores. The decomposition of the modified amino groups should enlarge clearances between Pd particles and the wall of the mesopores, which might provide a path for other gases. In contrast, the amino groups might be present although they must be partially decomposed during the hydrogen reduction process.

The gas permeation test at 573 K through APS-3 showed H_2 and CO_2 permeance gradually increased over the time course of the experiment and after 72 h they were 1.9×10^{-6} and 3.1×10^{-9} mol m^{-2} s^{-1} Pa^{-1}, respectively (Fig. 8). The H_2 selectivity was almost stable with time and was 610 after 72 h (Fig. 8). The H_2 selectivity was considerably increased by

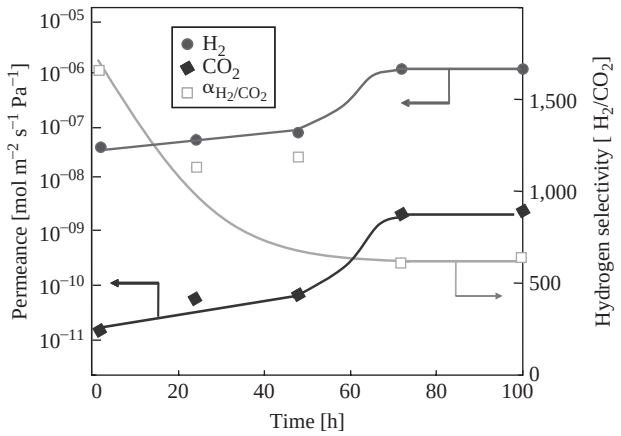

Fig. 8. Gas permeation properties of APS-3 at 373K: Feed gas, $H_2/CO_2 = 50/50$; $\Delta P = 150$ kPa.

electroless plating. This might be caused by densely packing the mesopores with Pd nanoparticles and it was found that electroless plating was an efficient way to encapsulate Pd particles in the silica layer. The gradual increase of permeance implies the membrane structure was slightly changed during the operation, perhaps through decomposition of modified amino groups and sintering of Pd nanoparticles. However, a decrease in selectivity was not observed, even after more than 100 h, indicating this membrane had good stability against hydrogen embrittlement although the reason for the increase of permeance remains unknown.

Gas permeation tests were conducted over membrane CD-1 at 373 and 573 K (Figs. 9a and 9b). The H_2 selectivity of CD-1 was 500 and the H_2 permeance was 1.0×10^{-7} mol m^{-2} s^{-1} Pa^{-1} after 24 h at 373 K. After 24 h at 573 K, the corresponding results were approximately 300 for the H_2 selectivity and 5.6×10^{-7} mol m^{-2} s^{-1} Pa^{-1} for the H_2 permeance. Although the CO_2 permeance slightly increased after 45 h, the performance of CD-1 was almost stable for more than 70 h at 573 K.

Microscopic collapse of the mesoporous silica framework might have occurred due to thermal stress. This could result in the decrease in hydrogen selectivity with increasing temperature because the thermal expansion rate of silica is much lower than that of α-alumina and palladium.

To reduce thermal stress damage to the Pd/silica composite layer, an intermediate silica layer was prepared on the α-alumina substrate by spin-coating of colloidal silica solution and calcination at 873 K before preparation of the mesoporous silica layer. The thickness of the Pd encapsulated membrane including the intermediate silica layer was approximately 5 μm, as measured by SEM.

Gas permeation testing was conducted at 573 K over this composite membrane with an intermediate layer (Fig. 10). The initial H_2 selectivity was more than 3,000 and H_2 permeance was 1.5×10^{-7} mol m^{-2} s^{-1} Pa^{-1}. This high selectivity could be caused

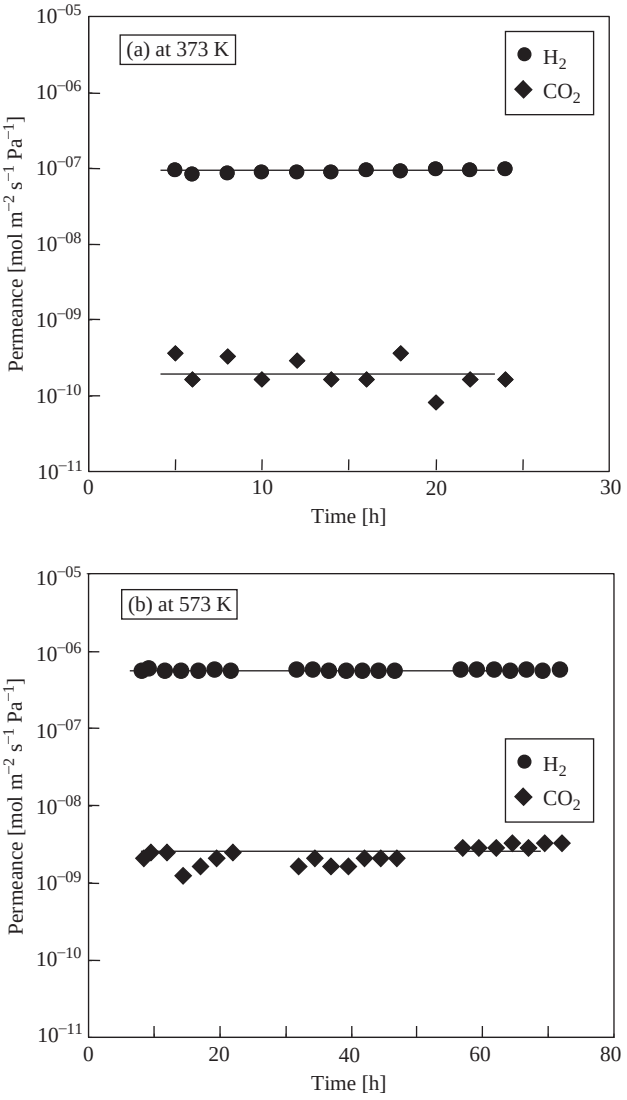

Fig. 9. Gas permeation properties of CD-1: Feed gas, $H_2/CO_2 = 50/50$; $\Delta P = 150$ kPa. (a) 373 K and (b) 573 K.

by a decrease in membrane defects, such as pinholes or cracks, achieved by denser packing of the Pd particles with the increase in membrane thickness. In contrast, the increase in membrane thickness caused a decrease in H_2 permeance. This is illustrated by the decreased rate of H_2 permeance, between with and without the intermediate layer, matching the increase of the membrane thickness. Although the H_2 selectivity slightly decreased to approximately 1,500 after 24–45 h, the membrane performance was stable from 45 h up to 120 h. This result clearly indicates the inclusion of an intermediate layer could improve thermal stability by relaxing thermal stress, as well as enhance H_2 selectivity by densification of the Pd/silica composite layer.

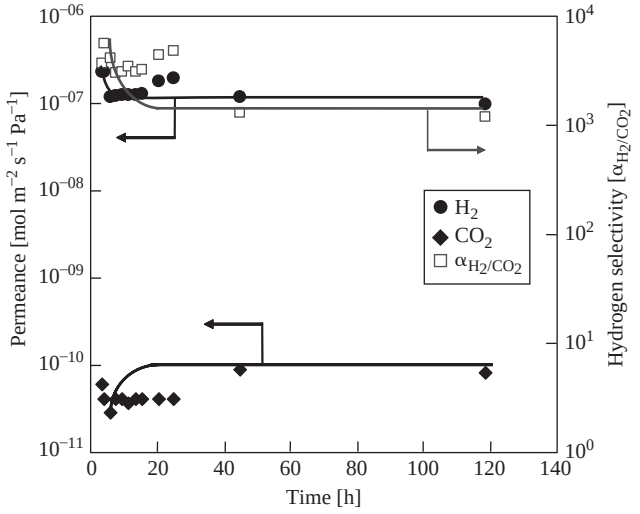

Fig. 10. Gas permeation properties of CD-2 at 573 K: Feed gas, $H_2/CO_2 = 50/50$; $\Delta P = 150$ kPa.

Fig. 11 shows hydrogen permeation flux of the CD-2 membrane as a function of pressure difference at 573 K. Here, P_h and P_l shows the hydrogen partial pressure in the feed side and permeate side, respectively. Hydrogen flux was increased with feed gas pressure. It appeared that gas permeation was by the solution–diffusion mechanism.

4. Conclusions

Pd encapsulated mesoporous silica membranes were prepared and their gas permeation properties were investigated. Pd impregnation into the

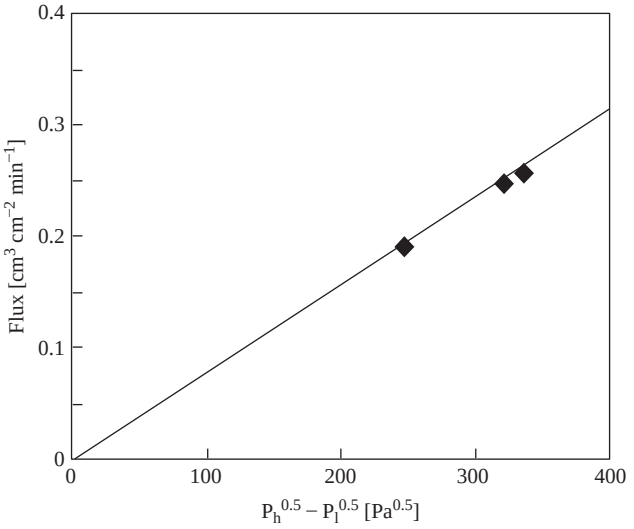

Fig. 11. Hydrogen permeation flux of the CD-2 membrane as a function of pressure difference at 573 K.

mesoporous silica membrane showed hydrogen selectivity and amine modification could enhance the selectivity because modified amino groups adsorbed Pd ions efficiently. Pd nanoparticles in the silica matrix allowed efficient hydrogen separation. The Pd layer could be synthesized within the silica layer regardless of differences in the Pd nuclei generation method. High hydrogen selectivity could be achieved for more than several tens of hours at 573 K by electroless plating, indicating that using the composite structure provides membrane stability as well as significantly reduction of Pd use for the membrane preparation. In addition, the inclusion of an intermediate layer improved membrane stability probably because of relaxation of thermal stress. This implies that the membrane stability could be improved further by applying materials that have high physical and chemical stability.

Acknowledgment

This work was financially supported by the Ministry of Economy, Trade and Industry (METI), Japan.

References

[1] S.N. Paglieri1 and J.D. Way, Sep. Purif. Methods, 31 (2002) 1–169.
[2] S. Adhikari and S. Fernando, Ind. Eng. Chem. Res. 45 (2006), 875–881.
[3] S.E. Nam and K.H. Lee, J. Membr. Sci., 192 (2001) 177–185.
[4] S.E. Nam and K.H. Lee, Ind. Eng. Chem. Res. 44 (2005) 100–105.
[5] S. Uemiya, N. Sato, H. Ando, Y. Kude, T. Matsuda and E. Kikuchi, J. Membr. Sci., 56 (1991) 303–313.
[6] D.A.P. Tanaka, M.A.L. Tanco, S. Niwa, Y. Wakui, F. Mizukami, T. Namba and T.M. Suzuki, J. Membr. Sci., 247 (2005) 21–27.
[7] S. Yan, H. Maeda, K. Kusakabe and S. Morooka, Ind. Eng. Chem. Res. 33 (1994) 616–622.
[8] J. Tong, L. Su, K. Haraya and H. Suda, J. Membr. Sci., 310 (2008) 93–101.
[9] D.A.P. Tanaka, M.A.L. Tanco, T. Nagase, J. Okazaki, Y. Wakui, F. Mizukami and T.M. Suzuki, Adv. Mater., 18 (2006) 630–632.
[10] D.A.P. Tanaka, M.A.L. Tanco, J. Okazaki, Y. Wakui, F. Mizukami and T.M. Suzuki, J. Membr. Sci., 320 (2008) 436–441.
[11] R.M. Rioux, H. Song, J.D. Hoefelmeyer, P. Yang and G.A. Somorjai, J. Phys. Chem. B., 109 (2005) 2192–2202.
[12] H.J. Shin, R. Ryoo, Z. Liu and O. Terasaki, J. Am. Chem. Soc. 123 (2001) 1246–1247.
[13] Y.S. Chi, H.P. Lin and C.Y. Mou, Appl. Catal. A., 284 (2005) 199–206.
[14] M.C. Carrión, B.R. Manzano, F.A. Jalón and I. Fuentes-Perujo, Appl. Catal. A., 288 (2005) 34–42.
[15] C. Senera, T. Dogua and G. Dogub, Microp. Mesop. Mater., 94 (2006) 89–98.
[16] Z.Z. Dai, S. Blomand, D. and D.A. Shen, J. Chem. Mater., 14 (2002) 965–968.
[17] H. Li, H. Lin, S. Xie, W. Dai, M. Qiao, Y. Lu and H. Li, Chem. Mater., 20 (2008) 3936–3943.
[18] Y. Sakamoto, K. Nagata, K. Yogo and, K. Yamada, Microp. Mesop. Mater., 101 (2007) 303–311.
[19] T. Kuji, Y. Matsumura, H. Uchida and T. Aizawa, J. Alloy. Comp., 330–332 (2002) 718–722.
[20] R.J.R. Uhlhorn, K. Keizer and A.J. Burggraaf, J. Membr. Sci. 46 (1989) 225–241.